# ROLL AMPLIFICATION OF SOLID ROCKET MOTOR IN LAPAN SOUNDING ROCKET (AMPLIFIKASI PUTAR GULING MOTOR ROKET PADAT DI ROKET SONDA LAPAN)

**O. Sudiana[1], P. Teofilatto[2]**
[1]Rocket Technology Center, LAPAN
[2]School of Aerospace Engineering, Sapienza University of Rome
[1]e-mail: sudiana.oka@gmail.com
Diterima : 6 Juni 2020; Direvisi : 16 Juni 2020; Disetujui : 20 Juli 2020

**ABSTRAK**

Roket sonda telah digunakan untuk penelitian ilmiah, dan di implementasikan dalam meteorologi dan studi atmosfer lapisan atas sejak akhir 1950-an. Roket sonda membawa muatan sub-orbital yang mengikuti lintasan terbang parabola dari peluncuran hingga pendaratan. Mendukung peta jalan pengembangan roket Peluncur Satelit, LAPAN telah meluncurkan Program roket sonda. Amplifikasi putar guling dari hasil produksi kecepatan putar yang tidak terduga terdeteksi selama dorongan dari roket sonda, meskipun sirip roket sayap dalam konfigurasi salib. Salah satu fenomena ini dapat dipengaruhi oleh aliran gas pada ruang pembakaran selama waktu pembakaran. Ide dasar dari penelitian ini adalah untuk memodelkan amplifikasi putar guling sebagai efek gerakan berputar-putar dari bagian gas buang yang berpartisipasi dalam dinamika rotasi dari roket dibandingkan dengan mengalir keluar langsung dari ruang bakar. Data penerbangan tersedia diperoleh dari hasil tes terbang terakhir tersaji. Data tersebut menunjukkan adanya amplifikasi putar guling yang signifikan ketika motor roket padat digunakan selama waktu pembakaran. Hasil pemodelan memiliki pendekatan yang baik bahwa Kehadiran bagian gas buang mempengaruhi amplifikasi putar guling yang tidak terduga.

Kata kunci: *Roket sonda, motor roket padat, amplifikasi putar guling*

**ABSTRACT**

Sounding rockets have been used for scientific research and implemented in meteorological and upper atmosphere studies since the late 1950s. Sounding rockets are sub-orbital carriers that follow a parabolic trajectory from launch to landing. Supporting the roadmap of Satellite Launch Vehicle development, LAPAN had launched The Sounding Rocket Program. A roll amplification of the unpredicted roll rate production was detected during the boost of the sounding rocket, despite the tail wings in cruciform configuration. One of this phenomenon can be influenced by the flow field of the combustion chamber during the boosting time. The basic idea of this research is to model the roll amplification effect as a swirling motion of exhaust gas portion that participate to the rotation dynamics of the rocket rather than immediately flow to the combustion chamber. Available flight data where is obtained from the last flight test presented. It showed the presence of a significant roll amplification when solid rocket motor is used during the burning time. The result has a good agreement that the presence of the exhaust gas portion influences the unpredicted roll amplification.

Keywords: *Sounding rocket, solid rocket motor, roll amplification.*

**NOMENCLATURES**

| | |
|---|---|
| $\rho_G$ | Exhaust gas density |
| $\rho_p$ | Propellant density |
| $\rho_{case}$ | Solid Rocket Motor case density |
| $L_p$ | Propellant length |
| $\Lambda$ | Propellant-exhaust gas density ratio |
| $\omega_0$ | Initial angular velocity |
| $\omega$ | Angular velocity at time $t$ |
| $\varepsilon$ | Propellant participatory |
| $r$ | Radius of propellant at time $t$ |
| $r_0$ | Inner radius of propellant |
| $r_{ext}$ | Outer radius of propellant |
| $r_f$ | Radius of case |
| $\Delta r$ | Thickness of case |
| $I_0$ | Moment of inertia of initial propellant |
| $I_{case}$ | Moment of inertia of case |
| $I_p$ | Moment of inertia of propellant at time $t$ |
| $I_G$ | Moment of inertia of exhaust gas at time $t$ |

## 1 INTRODUCTION

(Heru, 2013) wrote that based on the Decree of the Head of the National Institute of Aeronautics and Space (LAPAN) Number: 2 of 2011 concerning the organization and work procedures within the National Institute of Aeronautics and Space. The Deputy of Aeronautics and Space Technology responsible for carrying out the formulation and implementation of policies in the field of aerospace technology. The National Institute of Aeronautics and Space (LAPAN) priority programs as presented by the chairman of LAPAN are development of Satellite Launch Vehicle (SLV) and rocket propellant raw material. These priority programs are under the rocket technology center.

According to (Hardhienata, 2008), Fabrication and ground test of SLV will be planned in the near future, and hopefully it will launch at orbital flight phase. Failure in recent flight test allegedly was caused by lack of design, quality of fabrication, and the use of ballistic rocket type to launch.

Along with the development process of the sounding rocket program, some failures occurred in both static test and flight tests. In addition, the claims for highly flight distances and apogee are too early and have not been proven by comparing the results of calculations with actual flight tests.

The attitude and dynamics determination of the sounding rocket along flight trajectory has not been revealed before. Although it has passive stability when it flies, it is difficult to know the dynamics of sounding rocket behavior either in the ideal flight or in the anomalies (failures) flight trajectory.

However, a successful launch was verified on the flight test in December 2017. The sensitive amplification of the unpredicted roll rate production was detected during the boost of the sounding rocket.

This amplification also had been observed by (Stella, 2012). He wrote that during the launch of Mu-V, a Japan solid-propellant rocket system, roll torque was observed in all launches. The strength of the torque is typically very large immediately soon after the launch. Since many modern launchers, such as VEGA and ARES, European Launch Vehicle, are designed with solid rocket motor at first stage.

(Stella, 2012) also described that the phenomenon of roll amplification cannot be ignored since it repeats in the flight test. Moreover, the problem of the roll torque production cannot be neglected

because many modern launchers are designed with a solid rocket motor as theirfirst stage. The presence of roll amplification is usually stronger during the initial phase of flight.

## 2 ROLL AMPLIFICATION MECHANISM

(Waesche, & Summerfield, 1965) did the research in the solid combustion chamber. They found that the major unsolved problems in the field of solid propellant rockets is the phenomenon of combustion instability. This instability phenomenon can be found in encountered source of the self-amplification of a disturbance, the dynamic coupling of the oscillatory pressure field, and the combustion zone near the surface.

The result in Figure 2-1 has been done by (Di Mascio, et.al. 2014) showed the X-vorticity field in four different transversal planes (YZ) along the SRM axis, together with the relevant streamlines in the YZ planes. The presence of two counter-rotating shear layer structures aligned with the SRM axis that are responsible for the fluctuations of the flow field.

(Flandro, 1964) report that mentioned by (Stella, 2012) showed star-shaped cavities are capable of producing several levels of the roll amplification, depending upon the number of star-points. About concerning roll amplification generation, (Stella, 2012) took historical data reported from (Knauber, 1996) where star grain or finned type grain motors are the best candidates to produce the significant roll amplification.

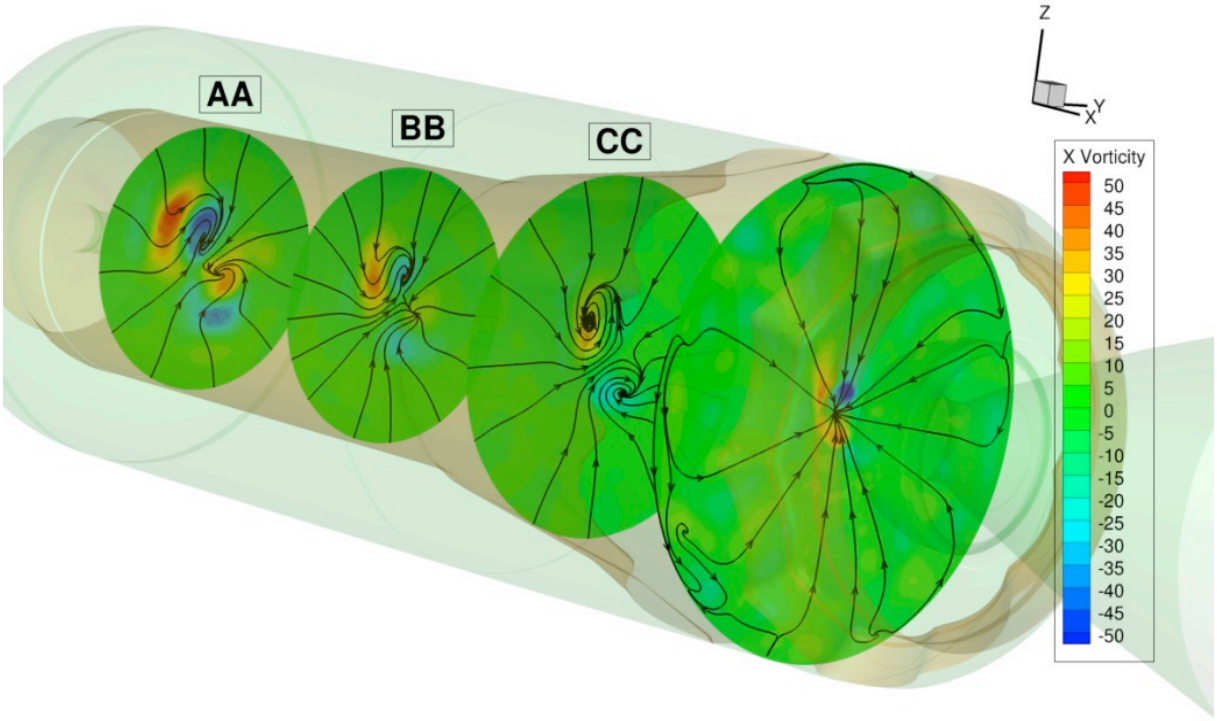


Figure 2-1: Vorticity of combustion and exhaust gas YZ Streamlines flow patterns (Di Mascio, A., et.al. 2014)

## 3 THE COMPUTATIONS OF PREDICT ROLL AMPLIFICATION

The basic idea is to model the roll amplification effect as a swirling motion of gas portion that participate to the rotation dynamics of the rocket (Figure 3-1.b) rather than the gas was immediately exit the combustion chamber (Figure 3-1.a and Figure 3-1.c)

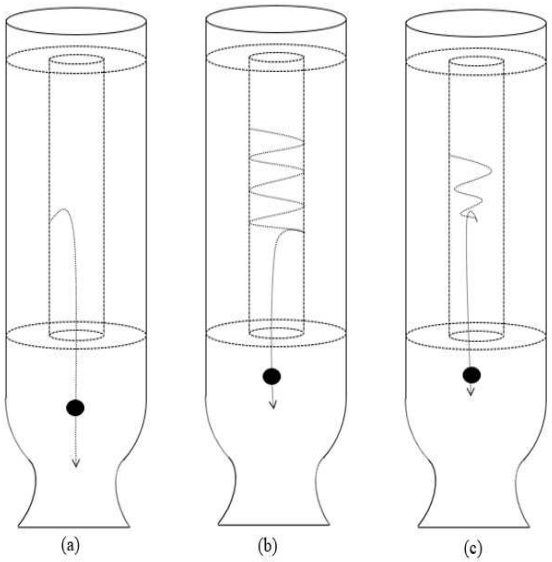


Figure 3-1: Gas portion flows the combustion chamber

If the external forces are zero, so that:

$$\frac{\mathrm{d}}{\mathrm{dt}}(\mathrm{I}\omega) = 0 \qquad (3\text{-}1)$$

The Eq. (3-1) above can be written as:

$$\mathrm{d}(\mathrm{I}\omega) = \mathrm{dI}.\,\omega + \mathrm{I}.\,\mathrm{d}\omega \qquad (3\text{-}2)$$

Then, it has to evaluate:

$$\mathrm{dI} = \mathrm{I}(\mathrm{t} + \mathrm{dt}) - \mathrm{I}(\mathrm{t}) \qquad (3\text{-}3)$$

At time $t = 0$, is before propulsion burning $r(0) = r_0$. And then at time $t$, the radius of the cylinder of the propellant grain is $r(t) = r$. The moment of inertia of the engine (case+grain) is the one of a hollow cylinder of radii $r_f + \Delta r$ and $r_0$, where $\Delta r$ is the thickness of the case.

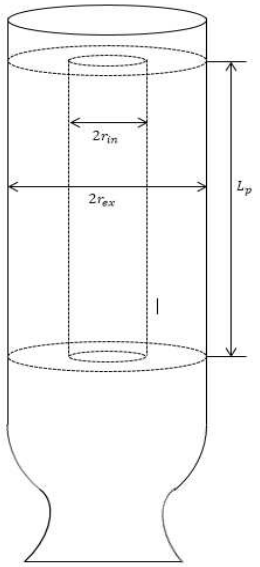


Figure 3-2: Propellant grain dimension

$I_0$ is the moment of inertia. While burning, the moment of inertia $I_0$ looses. The hollow cylinder of propellant has internal radius $r_{in}$ and external radius $r_{ex}$.

The moment of inertia of propellant equation can be obtain as:

$$I_p = \frac{1}{2} m_p \left(r_{ex}^2 + r_{in}^2\right) \qquad (3\text{-}4)$$

Since the propellant mass is consist of component mass density $\rho$ and volume $V$, it can be obtain as:

$$I_p = \frac{1}{2} \pi \rho_p L_p (r_{ex}^4 - r_{in}^4) \qquad (3\text{-}5)$$

when $\rho_p$ is the propellant density and $L_p$ is the length of cylinder.

This portion of propellant becomes gas leaving the combustion chamber through the nozzle. Suppose that a portion of such gas does not leave the grain surface immediately, but participate to the rotation of the rocket as if it is an added “rigid body” attached to the unburned grain. it must add the moment of this portion of gas to the rocket moment of motion.

The hypothesis is that the gas portion of the propellant participates to the rotational motion is equal to ε. Parameterε can be calculated from the case boundary as the following figure:

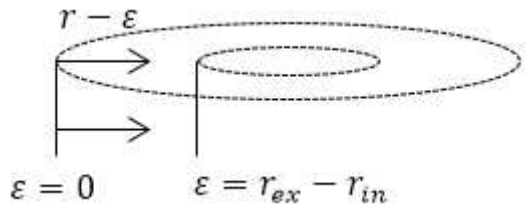


Figure 3-3: Propellant participatory

Then, if $r > \varepsilon$. It must have to add the hollow cylinder of gas:

$$I_G = \frac{1}{2}\pi\rho_G L_p(r^4 - (r-\varepsilon)^4) \tag{3-6}$$

where, $\rho_G$ is the density of exhaust gas.

Summing up all moment of inertia in rocket motor:

$$I(t) = I_0 - I_p + I_G \tag{3-7}$$

$$I(t) = I_0 - \tfrac{1}{2}\pi\rho_p L_p(r^4 - r_{in}^4) + \tfrac{1}{2}\pi\rho_G L_p(r^4 - (r-\varepsilon)^4) \tag{3-8}$$

$$I(t) = I_0 - \frac{1}{2}\pi\rho_G L_p\left[\frac{\rho_p}{\rho_G}r^4 - r^4 + \frac{\rho_p}{\rho_G}r_{in}^4 + (r-\varepsilon)^4\right] \tag{3-9}$$

Introducing:

$$\Lambda = \frac{\rho_p}{\rho_G}\left[{}^{kg}/_{m^3}\right] \tag{3-10}$$

Substitute the Eq. (3-10) into Eq. (3-9), can be written as:

$$I(t) = I_0 - \frac{1}{2}\pi\rho_G L_p[r^4(\Lambda-1) + \Lambda r_{in}^4 (r-\varepsilon)^4] \tag{3-11}$$

Now:

$$dI = I(t+dt) - I(t) \tag{3-12}$$

$$dI = \frac{\partial I}{\partial r}dr \tag{3-13}$$

$$dI = -\frac{1}{2}\pi\rho_G L_p[4r^3(\Lambda-1) + 4(r-\varepsilon)^3]dr \tag{3-14}$$

$$dI = -2\pi\rho_G L_p[r^3(\Lambda-1) + (r-\varepsilon)^3]dr \tag{3-15}$$

Then substitute the Eq. (3-11) and (3-15) into Eq. (3-2), it can be obtained as:

$$d(I\omega) = -2\pi\rho_G L_p[r^3(\Lambda-1) + (r-\varepsilon)^3]\omega d + \left[I_0 - \tfrac{1}{2}\pi\rho_G L_p[r^4(\Lambda-1) + \Lambda r_{in}^4 + (r-\varepsilon)^4]\right]d\omega \tag{3-16}$$

To take into account that the gas participating to the rocket rotation after a while leaves the combustion chamber, the first term:

$$2\pi\rho_G L_p(\Lambda r-\varepsilon)(r+dr-\varepsilon)^2\omega dr$$

Must be included in the balance up to $dr^2$, this term is equal to:

$$2\pi\rho_G L_p(\Lambda r-\varepsilon)(r-\varepsilon)^2\omega dr$$

Adding all the term, it becomes as:

$$2\pi\rho_G L_p\{[(\Lambda r-\varepsilon)(r-\varepsilon)^2] - [r^3(\Lambda-1) + (r-\varepsilon)^3]\}\omega dr + \left[I_0 - \frac{1}{2}\pi\rho_G L_p[r^4(\Lambda-1) + \Lambda r_{in}^4 + (r-\varepsilon)^4]\right]d\omega = 0 \tag{3-17}$$

Considering the $\{*\}$ term in $\omega dr$:

$$[(\Lambda r-\varepsilon)(r-\varepsilon)^2] - [r^3(\Lambda-1) + (r-\varepsilon)^3] = (\Lambda-1)[\varepsilon^2 r - 2\varepsilon r^2] \tag{3-18}$$

Then, substitute the $\{*\}$ term in $\omega dr$ which is described above to theEq. (3-17), can be written as:

$$2\pi\rho_G L_p\left[(\Lambda-1)[\varepsilon^2 r - 2\varepsilon r^2]\right]\omega dr + \left[I_0 - \frac{1}{2}\pi\rho_G L_p[r^4(\Lambda-1) + \Lambda r_{in}^4 + (r-\varepsilon)^4]\right] d\omega = 0 \quad (3\text{-}19)$$

Then the Eq. (3-19) can be written as:

$$2\pi\rho_G L_p\left[(\Lambda-1)[2\varepsilon r^2 - \varepsilon^2 r]\right]\omega dr = \left[I_0 - \frac{1}{2}\pi\rho_G L_p[r^4(\Lambda-1) + \Lambda r_{in}^4 + (r-\varepsilon)^4]\right] d\omega$$

$$\frac{d\omega}{\omega} = 2\pi\rho_G L_p(\Lambda - 1)\frac{2\varepsilon r^2 - \varepsilon^2 r}{I_0 - \frac{1}{2}\pi\rho_G L_p[r^4(\Lambda-1) + \Lambda r_{in}^4 + (r-\varepsilon)^4]}\, dr \quad (3\text{-}20)$$

Integrating the Eq. (3-20), will be obtained as:

$$\frac{\ln\omega}{\omega_0} = 2\pi\rho_G L_p(\Lambda - 1)\int_{r_0}^{r}\frac{2\varepsilon r^2 - \varepsilon^2 r}{I_0 - \frac{1}{2}\pi\rho_G L_p[r^4(\Lambda-1) + \Lambda r_{in}^4 + (r-\varepsilon)^4]}\, dr \quad (3\text{-}21)$$

## 4 RESULT AND ANALYSIS

The results from the data recording on the sounding rocket flight test, in spite of flying without any problems, an anomaly occurred on the gyroscope readings can be seen in Figure 4-1

It appears in Figure 4-1 that roll rate increases significantly in negative value until the peak when burning end and then headed to equilibrium even though it still rolling occurs during the flight.

A temporary hypothesis of an amplitude waves occur in the combustion chamber during propellant combustion. The gas portion around the combustion chamber may affect tothe rotational motion of the rocket.

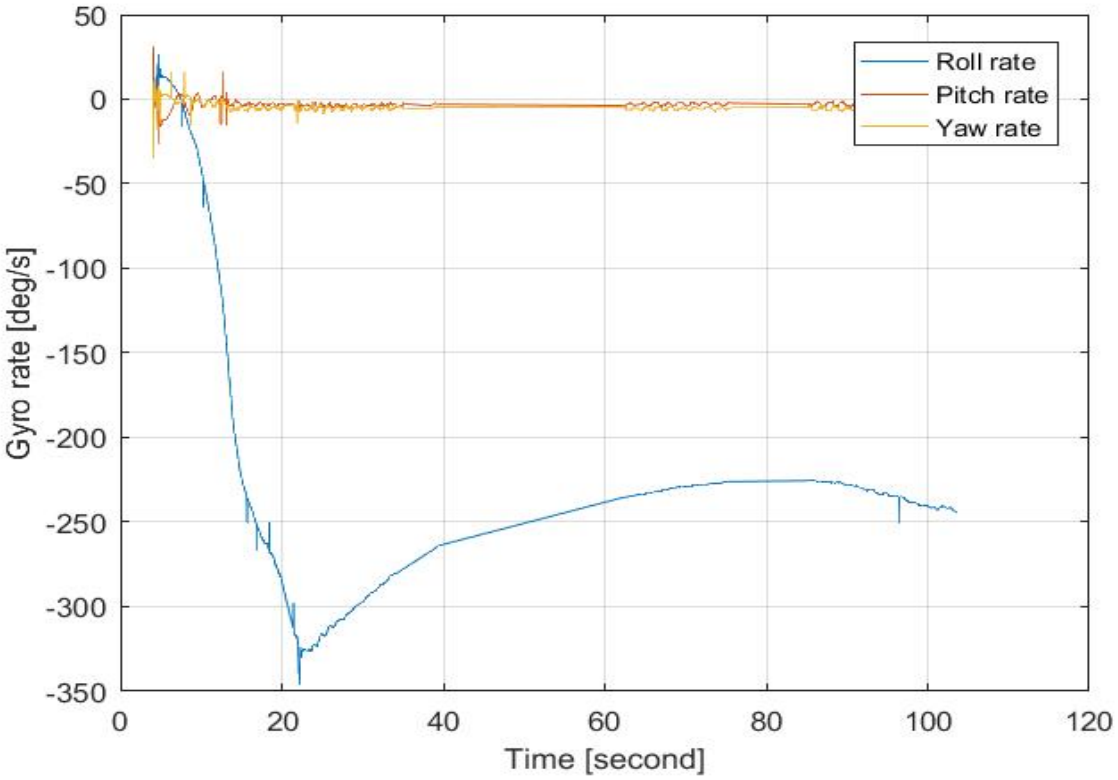


Figure 4-1: Gyroscope readings in flight test (Salman, 2017)

The geometrical dimensions and properties of the solid rocket motor are taken in this roll amplification calculation, as follows:

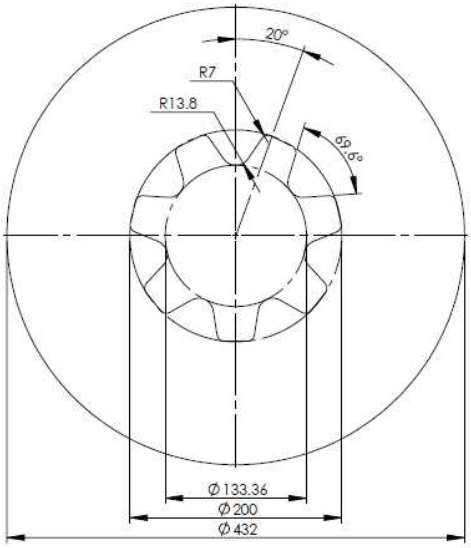


Figure 4-2: Propellant grain dimension (Badi and M.H. Aulia, 2015)

Table 4-1: PROPELLANT GEOMETRY AND PROPERTIES (Badi and Aulia, 2015; Wibowo, 2018)

| | |
|---|---|
| Propellant length | $L_p = 3.7\ m$ |
| Propellant external radius | $r_{ex} = 0.216\ m$ |
| Propellant av. Internal radius | $r_{in} = 0.083\ m$ |
| Propellant grain density | $\rho_p = 1635\ kg/m^3$ |

The result of Solid Rocket Motor combustion in the combustion chamber produces the exhaust gas with the following contents:

Table 4-2: EXHAUST GAS PROPERTIES (Cai, Thakre, & Yang, 2008)

| Gas properties | Mol/100g |
|---|---|
| $CO_2\ (CarbonDioxide)$ | 0.83 |
| $CO\ (CarbonMonoxide)$ | 0.88 |
| $H_2O\ (water)$ | 0.37 |
| $HCl\ (HydrogenChloride)$ | 0.58 |
| $H_2\ (Hydrogen)$ | 1.17 |
| $N_2\ (Nitrogen)$ | 0.29 |
| $Al_2O_3\ (AluminiumOxide)$ | 0.35 |

At Combustion Pressure = 7MPa; Combustion Temperature = 3533 K

From Figure 4-1, it shows that the rocket has a prefix roll on 45 degrees which triggers amplification. The rocket is rolling until it reaches a roll rate peak of 330 deg/sec, more than 7 times from the initial roll. Afterwards, the rocket is experiencing a slowdown until it reaches equilibrium with an average roll rate on 240 deg/sec.

According to the model in numerical simulation, we get a factor slightly to 7 times of initial roll rate. In fact,the experience in previous flight test reveals thefactor was closely to 7.5 times.

The model considers a cylindrical slot in the grain geometry to simplify thenumerical simulation, instead of star-shaped slot geometry which was used on the actual rocket shown in Figure 4-2.

However, according to numerical test that had been done by (Stella, 2012), the geometry of the grain is rather important. For instance, the different geometry of the grain in Stella has produced very different result. Figure 4-4 and Figure 4-5 depict the result that the higher ratio of the propellant slot the higher roll torque.

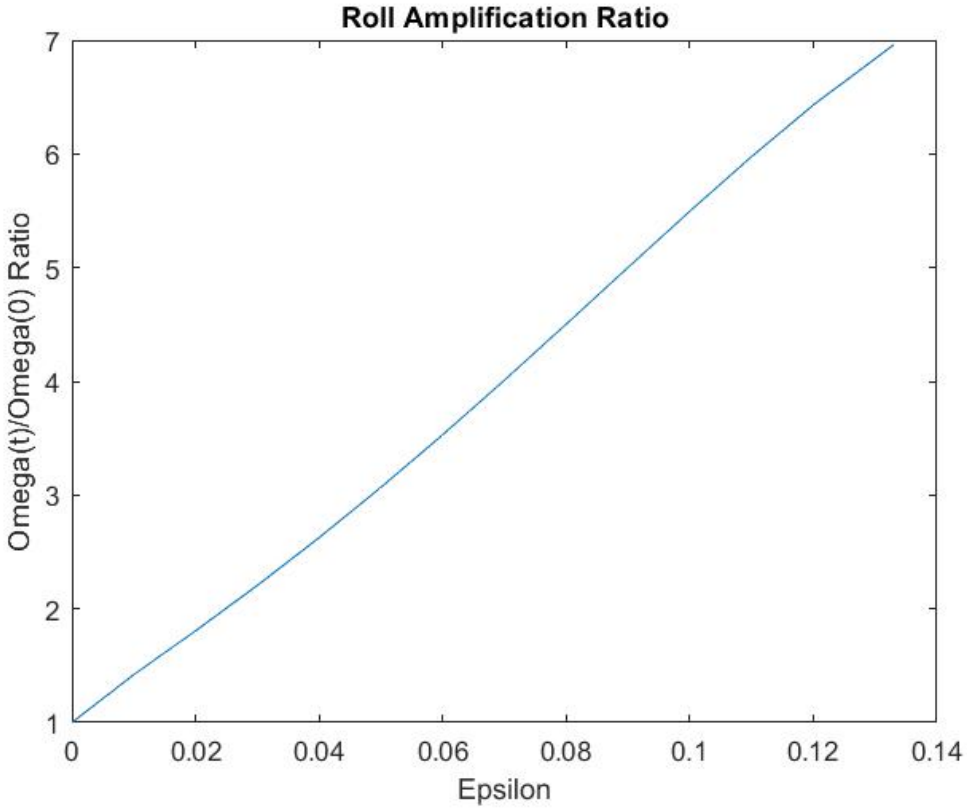


Figure 4-3: Roll amplification rasio

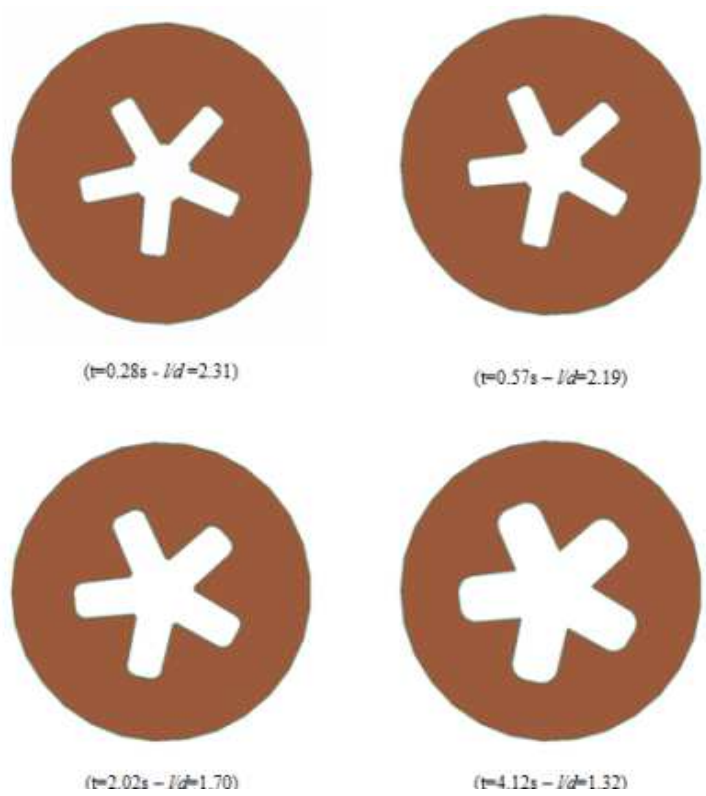


Figure 4-4: Ratio of propellant slot (Stella, 2012)

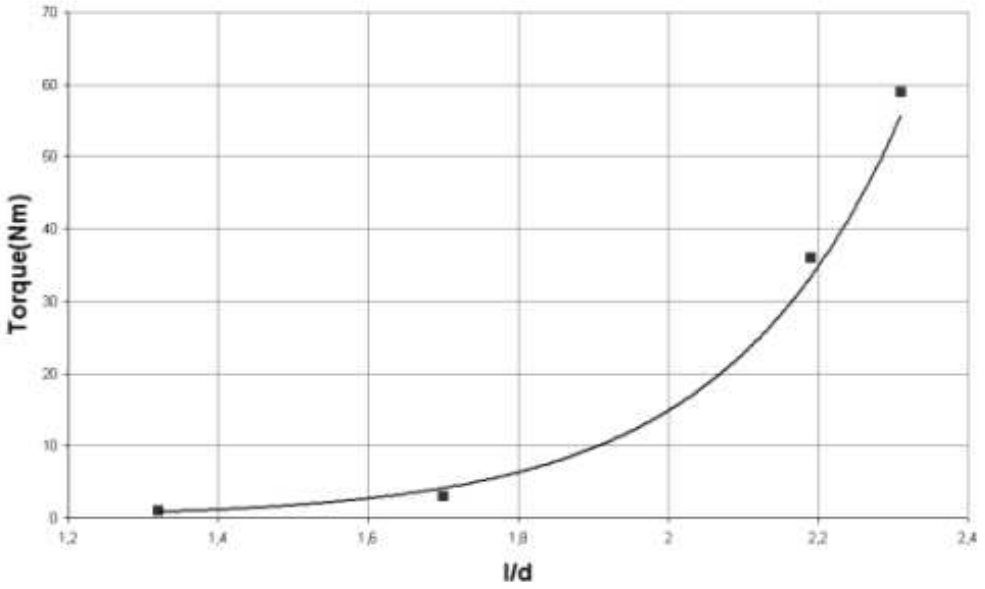


Figure 4-5: Roll torque as a function of slot aspect ratio (Stella, 2012)

Summarizing, numerical simulation models and experimental tests can improve the understanding of the roll anomaly and suggest solutions in next future.

## 5 CONCLUSIONS

The computation and analysis results of roll amplification outline are able to describe the events in the rocket motor combustion chamber during the flight test.

Star-shaped cavities are capable of producing several levels of roll amplification, depending upon the number of star-points. The model considers cylindrical slot in the grain geometry to simplify the numerical simulation, instead of star-shaped slot geometry. However, the geometry of the grain is rather important. The different geometry of the grain produces very different result. Higher ratio of propellant slot increased the roll torque higher.

The numerical simulation result isclosely enough to represent roll amplification on the experiment flight test and may predict the roll amplification since the production of sounding rocket may use similar treatment.

The analysis result can help in designing of future solid rockets and advanced control systems to overcome these problems. Numerical models and experimental tests can improve the understanding of the roll anomaly and suggest solutions in next future.

## ACKNOWLEDGEMENTS

Foremost, I would like to express my sincere gratitude to Prof. Paolo Teofilatto and co-supervisor Stefano Carletta, PhD cand. for the continuous support of my research, for their patience, motivation, enthusiasm, and immense knowledge. Their guidance helped me in all the time of research and academic. Special thanks addressed to Kemenristekdikti through RisetPRO program for financial support in doing this research. Also thanks to Rocket Technology Center, LAPAN Indonesia which has provided supporting

data for my research, which is very useful for completing the research.

**CONTRIBUTORSHIP STATEMENTS**

O. Sudiana is the main contributor and do the numerical simulation analysis in this research, while P. Teofilatto contributes to a mission analysis.

**REFERENCES**

Badi and M.H. Aulia. (215). *RBX450-UT Dimension*. Technical Report. LAPAN files.

Cai, W., Thakre, P., & Yang, V. (2008). *A model of AP/HTPB composite propellant combustion in rocket-motor environments*. Combustion Science and Technology, 180(12), 2143-2169.

Di Mascio, A., et.al. (2014). *Numerical Simulation of 3D Unsteady Flowfield in Aft-Finocyl Solid Rocket Motor*. In *50th AIAA/ASME/SAE/ASEE Joint Propulsion Conference* (p. 4015).

Engineering ToolBox, (2003). *Gases - Densities*. vailable at: https://www.engineeringtoolbox.com/gas-density-d_158.html [Accessed September 15, 2019].

Ferretti, V., et. al. (2010,). *Numerical simulations of acoustic resonance of Solid Rocket Motor*. In *46th AIAA/ASME/SAE/ASEE Joint Propulsion Conference & Exhibit* (p. 6996).

G. A. Flandro (1964).*Roll Torque and Normal Force Generation in Acoustically Unstable Rocket Motors*. AIAA Journal, 2.

Hardhienata, S. (2008). *The Program of Development of Aerospace Technology in Indonesia*. SIPTEKGAN XII-2008 pp 731-738. ISBN: 978-979-1458-19-1.

Heru. (2013). *Strategic Plan of the Deputy of Aeronautics and Space Technology 2010-2014*. LAPAN files.

R. N. Knauber (1996).*Roll Torque Produced by Fixed–Nozzle Solid Rocket Motors*. J. Spacecraft and Rockets, 33 (6).

Salman. (2017). *RX450 Flight Test*. Technical Report. Rocket Technology Center, LAPAN.

Stella, F. (2012). *Roll torque prediction in SRM: practical applications*. 63rd International Astronautical Congress.

Waesche, R. H., & Summerfield, M. (1965). *Solid Propellant Combustion Instability: Oscillatory Burning of Solid Rocket Propellants (No. AMS-751)*. PRINCETON UNIV NJ DEPT OF AEROSPACE AND MECHANICAL SCIENCES.

Wibowo, Heri Budi. (2018). *Current solid propellant research and development in Indonesia and its future direction*. Journal of Physics: Conference Series. 1130. 012027. 10.1088/17426596/1130/1/012027.

.